Proc. Natl. Acad. Sci. USA
Vol. 91, pp. 12268–12272, December 1994
Biophysics

Motility voltage sensor of the outer hair cell resides within the lateral plasma membrane

GUOJIE HUANG AND JOSEPH SANTOS-SACCHI*

Sections of Otolaryngology and Neurobiology, Yale University School of Medicine, New Haven, CT 06510

Communicated by Jozef J. Zwislocki, August 25, 1994

ABSTRACT **The outer hair cell (OHC) from the organ of Corti is believed to be responsible for the mammal's exquisite sense of hearing. A membrane-based motile response of this cell underlies the initial processing of acoustic energy. The voltage-dependent capacitance of the OHC, possibly reflecting charge movement of the motility voltage sensor, was measured in cells during intracellular dialysis of trypsin under whole cell voltage clamp. Within 10 min after dialysis, light and electron microscopic examination revealed that the subplasmalemmal structures, including the cytoskeletal framework and subsurface cisternae, were disrupted and/or detached from adjacent plasma membrane. Dialysis of heat-inactivated trypsin produced no changes in cell structure. Simultaneous measures of linear and nonlinear membrane capacitance revealed minimal changes, indicating that contributions by subsurface structures to the generation of the nonlinear capacitance are unlikely. This study strongly suggests that voltage-dependent charge movement in the OHC reflects properties of the force generator's voltage sensor and that the sensor/motor resides solely within the lateral plasma membrane.**

The mammalian outer hair cell (OHC) possesses a unique transmembrane voltage-driven mechanical response that can occur at acoustic frequencies (1–5). This mechanical activity is believed to underlie the enhanced ability of the inner ear to detect and analyze sound (6) and is especially interesting since it is not directly dependent upon Ca^{2+} or metabolic substrates (3, 7, 8). A nonlinear charge movement, or corresponding voltage-dependent capacitance, has been observed in this cell and it probably reflects the activity of the motility voltage sensor, as many of its characteristics and those of the mechanical response coincide (9–12). Recently, the mechanical response and the extent of the nonlinear capacitance have been mapped along the central portion of the cylindrical OHC (13, 14); each corresponds roughly to the extent of subplasmalemmal structures, the cortical network of cytoskeletal filaments, and the subsurface cisternae. It is of interest to determine whether such structures contribute to the motile mechanism or nonlinear charge movement or if the cell's plasma membrane alone is responsible for these phenomena. The experiments of Kalinec *et al.* (15) have shown that intracellular dialysis of trypsin does not abolish OHC membrane movements. However, no electron microscopic analysis of the effects of the trypsin treatment was performed, so it is unclear whether the plasma membrane was totally isolated from intracellular structures in their experiments. We report here that following intracellular trypsin treatments, most of the plasma membrane is isolated from subsurface structures as evidenced electron microscopically. Furthermore, the nonlinear charge movement remains intact during such treatments, indicating that the motility voltage sensor, as well as the motor, reside within the plane of the OHC plasma membrane.

The publication costs of this article were defrayed in part by page charge payment. This article must therefore be hereby marked "*advertisement*" in accordance with 18 U.S.C. §1734 solely to indicate this fact.

MATERIALS AND METHODS

General. Guinea pigs were euthanized with halothane overdose. The isolated organ of Corti was treated with collagenase (0.3 mg/ml for 10 min) and triturated gently within a polyethylene pipette in medium 199 with Hanks' salts (GIBCO). The OHC-enriched supernatant was then transferred to a 700-μl perfusion chamber. Experiments were performed at room temperature (22°C).

Electrical Recording. OHCs were whole cell voltage clamped with a Dagan 8900 patch clamp amplifier at a holding potential of −80 mV. Cells were bathed in a modified Leibovitz medium (in mM: NaCl 110, KCl 5.37, $CoCl_2$ 2, $MgCl_2$ 1.48, tetraethylammonium chloride 20, CsCl 20, Hepes 5, and dextrose 5; 300 mosM, pH 7.2) in order to block ionic conductances. Pipette solutions were composed of (mM) CsCl 140, EGTA 10, tetraethylammonium chloride 5, $MgCl_2$ 2, and Hepes 5 (300 mosM, pH 7.2). Gigohm seals were obtained at the middle portion of the lateral wall. In order to introduce trypsin into the cell, relatively large patch pipette tips were used (1.5- to 2-μm inner diameter; series resistance, 2–3 MΩ). For trypsin treatments, 300 μg of trypsin (source: bovine pancreas, M_r 23,281; Calbiochem) was dissolved in 1 ml of pipette solution and the osmolarity and pH were readjusted to 300 mosM and pH 7.2. As a control, heat-inactivated trypsin (enzyme pipette solution heated for 30 min in 56°C water bath) was also used. Electrode capacitance was compensated after gigohm seal formation, and series resistance compensation was used in whole cell configuration. A modified version of Clampex (Axon Instruments, Burlingame, CA) was used to apply voltage stimuli and collect data that were saved on disk for off-line analysis. Current was filtered at 5 kHz with an eight-pole Bessel filter. All experiments were videotaped.

Three methods were used to evaluate the effects of trypsin treatment on cell capacitance. The first method simply measured cell capacitance near the cell's normal *in vivo* resting potential. The cell was nominally held at −80 mV and a −10 mV step command voltage (4 ms) was applied repeatedly over time. At this potential both linear and a substantial amount of nonlinear capacitance contributes to the generation of a transient capacitive current (12). From averaged (×20) current records, an on-line analysis of membrane capacitance (C_m), membrane resistance (R_m), and series resistance (R_s) was performed and saved to disk. The transient analysis calculations have been published elsewhere (16).

The second method evaluated the voltage dependence of nonlinear capacitance using a voltage stair protocol. The technique has been fully described elsewhere (14). Briefly, the cell was stair-stepped from a holding potential of −170 mV to voltages between −160 mV and +50 mV, in increments of 10 mV. From each step response, C_m, R_m, and R_s were calculated as a function of membrane voltage. The

Abbreviation: OHC, outer hair cell.

*To whom reprint requests should be addressed.

measured membrane capacitance has two components, a linear one, which is a function of the total cell membrane area, and a nonlinear one, which is a measure of the charge movement of the motility voltage sensor. The total membrane capacitance (C_m) at any given voltage is the sum of the linear (C_{lin}) and nonlinear (C_v) capacitance. The nonlinear capacitance (C_v) can be described as the first derivative of a two-state Boltzmann function relating nonlinear charge movement to voltage, and such a fit provides estimates of the charge characteristics, including the voltage at half-maximal nonlinear charge transfer (V_h), and charge valence (z) (see Fig. 3 and ref. 14 for further details). Measures were made at 1- to 5-min intervals following whole cell configuration.

The third method was used to overcome potential harmful effects of the large voltages of the stair protocol. To estimate maximal nonlinear capacitance, a software tracking protocol using step analysis was developed to monitor peak capacitance by iteratively adjusting the holding potential to maintain the cell at V_h—i.e., the voltage at which nonlinear capacitance is greatest. Should V_h change during an experiment, the tracking technique, utilizing −10 mV steps, will continue to determine peak capacitance.

Electron Microscopy. Following single cell capacitance evaluations, primary fixation was accomplished by slowly perfusing the recording chamber with 0.75% glutaraldehyde in 0.1 M sodium cacodylate buffer with 2 mM $CaCl_2$ (300 mosM, pH 7.3). The perfusion rate was about 0.05 ml/min in order to minimize distortion of the cell. After perfusion for 30 min, cells were washed with buffer for 10 min and released from recording pipettes by gently breaking the tip on the chamber floor. To continue processing without losing the cell, a microchamber embedding method was devised. A polypropylene disposable pipette (Fisher) was heated and pulled to approximately 20- to 30-μm internal radius and 10- to 15-μm wall thickness. Under a dissecting microscope, the tube was shoed to the tip of a glass pipette. Cells were gently sucked into the microchamber, and the microchamber was affixed to the bottom of a new perfusion dish. Cells were postfixed with 1% OsO_4 in 0.1 M sodium cacodylate buffer (pH 7.3, 300 mosM) for 30 min, followed by dehydration in a graded series of ethanol up to 100%. Cells were stained with 2% uranyl acetate (while in 70% ethanol) for 30 min in the dark.

Poly Bed 812 was prepared according to the Mollenhauer mixture 1 formula (Polyscience). Three changes in graded concentrations of Poly Bed 812 (epoxy resin/ethanol, 1:3, 1:1, 3:1; 4 hr each) were followed by three changes in pure Poly Bed 812 (4 hr each). Polymerization was at 60°C overnight. The plastic microchamber was then cut out and reembedded in an Epon block. Ultrathin sections (70–80 nm) were taken at various points through the cell extent, placed on Formavar-coated 200-mesh copper grids, and stained with uranyl acetate (10 min) and lead citrate (2 min). Sections were observed with a Phillips 300 electron microscope at 60 kV.

RESULTS

During the course of whole cell electrical recording, trypsin enters the OHC and alters the cell's normal cylindrical structure. In a group of 15 OHCs, simultaneous capacitance measures were obtained at a nominal holding potential of −80 mV. Within 3–23 min (10.2 ± 6.7 min; mean ± SD), these cells were transformed into spherical structures, which appeared at the light microscopic level to have undergone an involution and separation of the cell's subplasmalemmal structures from the plasma membrane. Fig. 1 illustrates the progression of this phenomenon. After the OHCs became fully spherical, the cells were fixed for electron microscopy. However, in some cells that were not fixed, continued dialysis eventually caused dissolution of the nucleus and much of the cuticular plate. Although dramatic alterations in cell structure were observed, C_m at −80 mV did not decrease, as might have been expected if subplasmalemmal structures were requisite for the nonlinear capacitance component. Average data are presented in Fig. 2 and show that C_m actually increased in this sample from an initial value of about 35 pF to 39 pF. R_m decreased during the recording to about 75% of the initial 103 MΩ average. The electrode series resistance remained constant at about 6 MΩ, indicating that efficient dialysis was maintained throughout the recording period.

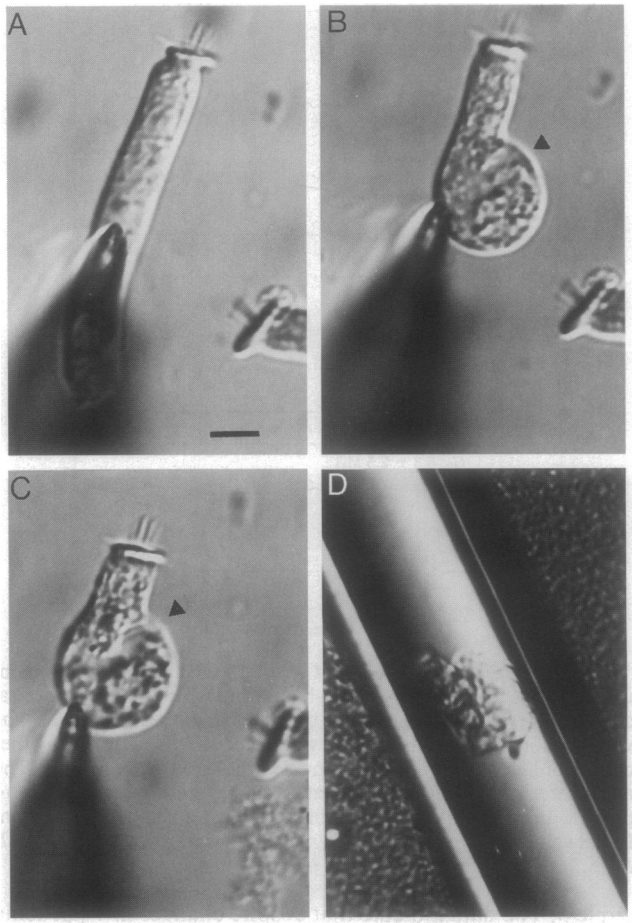

FIG. 1. Light microscopy of an OHC during the course of trypsin treatment and capacitance measurement, illustrating the loss of the cell's cylindrical shape and involution of intracellular cortical structures. (*A*) Cell 5 min after established whole cell configuration. (*B* and *C*) At the 12th and 16th min, respectively. The arrowheads indicate the area where the cortical structures began separation from the plasma membrane. This cell eventually became fully spherical at the 20th min and was then fixed. (*D*) Cell within a plastic microchamber, prior to embedding. (Bar = 10 μm.)

During capacitance measures obtained at a fixed holding potential, it is possible that either holding potential changed, as a consequence of changes in the ratio of series resistance to membrane resistance (the voltage divider effect), or V_h changed, as a consequence of trypsin treatment. Such occurrences could account for the observed change in total membrane capacitance in Fig. 2. In fact, using the stair-step voltage protocol, it was determined that V_h shifts occurred in some cells. Fig. 3 illustrates the data obtained using the stair protocol. The results from a single cell are presented in Fig. 3 *Upper* and the average capacitance for 9 cells is presented in Fig. 3 *Lower*. In each panel, the voltage-dependent capacitance was measured within a minute after cell entry (closed circles) and after the cells had become spherical (open

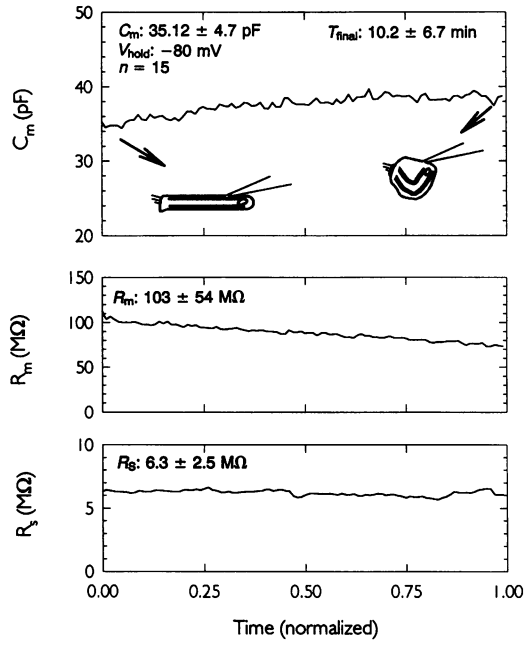

FIG. 2. Average C_m, R_m, and R_s of 15 OHCs during treatment with trypsin. The cells changed shape from cylindrical to spherical during the trypsin treatment, but the time to reach a spherical shape varied among cells, with an average time of 10 ± 6.7 min. Two other cells spontaneously burst at the nuclear pole during recording. The data were normalized by decimation along the time dimension to provide an end point corresponding to the time of sphere formation. Initial values were as follows: C_m, 35.12 ± 4.7 pF; R_m, 103 ± 54 MΩ; R_s, 6.3 ± 2.5 MΩ. Note a slight *increase* in C_m.

circles). The data indicate that despite changes in V_h in some cells (average shift of −11 mV; see legend to Fig. 3), voltage-dependent characteristics of the nonlinear capacitance remained near normal, as did peak capacitance values. We have recently observed that a reduction of membrane tension, caused by reduced intracellular pressure, increases nonlinear capacitance and shifts V_h in the negative direction—up to a limiting voltage approaching the membrane potential of OHCs *in vivo*—namely, −70 mV (S. Kakehata and J.S.-S., unpublished observations). We speculate that trypsin treatment reduces tension on the membrane by destroying cortical cytoskeletal interactions with the membrane, causing a negative shift of V_h, and probably accounting for the increase of OHC C_m observed at a holding potential of −80 mV (Fig. 2).

We also confirm the results of Kalinec *et al.* (15), since we observe robust mechanical responses under this voltage protocol despite the fact that the plasma membrane appears divorced from intracellular structures. Nevertheless, the motility that remains in trypsin-treated cells is not the same as in normal cells. This results from the disruption of the cell's normal cytoarchitecture and mechanical properties that provide for the normal longitudinal length changes. Thus, despite the fact that the cell continues to respond to voltage changes by modifying its shape, motility characteristics (e.g., frequency response) may be altered and require further evaluation.

The stair protocol subjects the cells to very large, rapid voltage changes, which, over repeated application, tend to damage the cell or electrode seal. This is especially the case for trypsin-treated cells, which are by definition already compromised. In fact, many spherical cells were lost during such collections. In 19 cells that underwent the stair protocol, the electrode seal was lost in 10 cells, and in another 2 cells the membrane burst at locations remote from the electrode location, near the nuclear pole. Therefore, estimates of peak

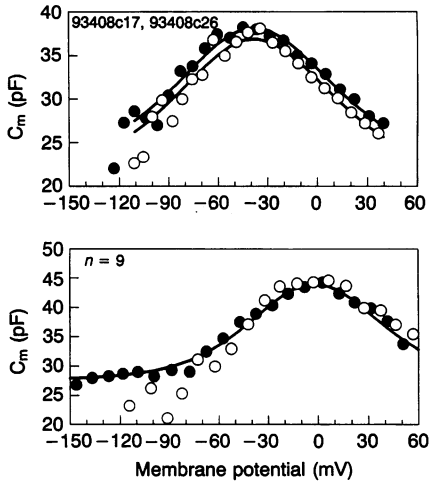

FIG. 3. Voltage-dependent capacitance of OHCs measured with the stair-step protocol during trypsin treatment. The voltage-dependent capacitance rides upon a linear membrane capacitance ($C_m = C_v + C_{lin}$). ●, C_m recorded immediately after the establishment of whole cell configuration; ○, data obtained after the OHCs became spherical. During stimulation, OHCs responded with robust motility, either before or after trypsin effects were evident. (*Upper*) Results from a single OHC. In this case, the voltage at peak capacitance (V_h) remained constant before and after trypsin treatment. Fits of the data to the first derivative (with respect to membrane voltage) of a two-state Boltzmann function [$Q(v) = Q_{max}/1 + \exp(-ez(V_m - V_h)/kT)$, where e, k, and T have their usual meanings] are indicated by the solid lines, with an additional linear capacitance added (C_{lin}). For the control condition (●), $z = 0.82$, $Q_{max} = 1.97$ pC, $V_h = -38$ mV, and $C_{lin} = 22.4$ pF. The fit through the open circles is the same, with C_{lin} reduced by 1.25 pF. (*Lower*) Averaged results from nine cells. The voltage at peak capacitance (V_h) was found to vary among cells. To average the capacitance measures from different cells, all functions were shifted along the voltage axis so that V_h resided at 0 mV. Since the actual voltage at each step differed for each cell because of differences in the ratios of R_s to R_m, the data were binned into 10 mV ranges. Both voltages and capacitance values were averaged within bins. Symbols as above. The fit through the closed circles provided average parameters of $z = 0.98$, $Q_{max} = 1.7$ pC, and $C_{lin} = 27.7$ pF. The actual average voltage at peak capacitance (V_h) for the control condition was −15 mV and after trypsin effects were evident, −26 mV. The capacitance values after trypsin treatment (○) are similar (or slightly increased) to the control except at hyperpolarized voltage steps, where it appeared that membrane characteristics became unstable.

capacitance were also obtained by the tracking technique described in *Materials and Methods*. Fig. 4 provides an example of a cell that was monitored during trypsin treatment well beyond the point where it reached a fully spherical shape. Peak capacitance remained relatively constant throughout the recording period ($n = 7$).

Fig. 5 presents a low-power electron micrograph of an OHC after trypsin had caused the cell to become spherical. The striking feature of the trypsin treatment was a separation of the plasmalemma from subsurface cisternae and cortical cytoskeleton. Vast amounts of plasma membrane appeared free of any subsurface interactions. In higher magnification

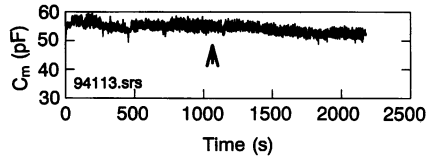

FIG. 4. Peak capacitance (C_m) of an OHC that was monitored with the tracking procedure during trypsin treatment (see text). The arrow indicates the point at which the cell became fully spherical. Note that peak capacitance remains nearly constant in this example.

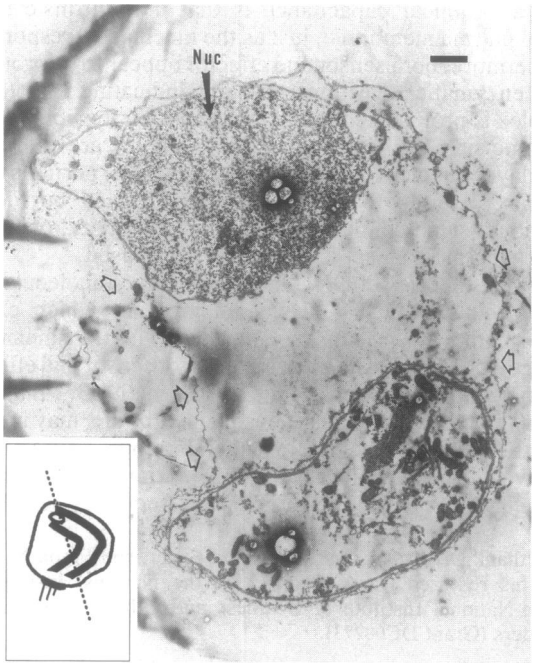

FIG. 5. Low-power electron micrograph of a trypsin-treated OHC within a microchamber. Five minutes after the initiation of recording the cell became spherical and was fixed. Arrows point to the plasmalemma, which is divorced from intracellular structures. (*Inset*) Schematic illustrating the section orientation through the spherical cell. Note, in the electron micrograph, on one side of the cell the nucleus (Nuc) is sectioned, and on the other side more apical regions are sectioned. (Bar = 1 μm.)

views (Fig. 6), it was apparent that the cytoskeletal attachments between the plasma membrane and subsurface cisternae were digested by the enzyme, allowing the cisternae to peel away from the plasma membrane. In five cells successfully recovered for electron microscopy, the bulk of plasma membrane was cleanly isolated, indicating that the capacitance measures reflected simply the intrinsic properties of plasma membrane components.

DISCUSSION

The OHC possesses a unique ability to alter its length in response to electrical stimulation (1). The driving force for this phenomenon is currently considered to be transmembrane voltage (3, 5), and in line with this hypothesis is the demonstration of a gating charge or nonlinear capacitance in the OHC that is associated with the mechanical event (9, 11). The charge displacement may reflect the movement of a proteinaceous motor's voltage sensor, just as voltage sensors of ionic channels demonstrate transient charge movements during channel gating. This contention is based upon similarities between some of the characteristics of the gating charge movement and the mechanical response in the OHC (12, 17). For example, the time course of gating charge movement and OHC motility are similar, and factors affecting the gating charge also are reflected in the motion of the cell. Another indication is that the extent of the charge movement along the length of the cell corresponds to those regions of the cell that are mechanically active (14). Furthermore, both motor activity and nonlinear charge movement are discretely distributed along the cell body and can be activated independently in different regions of the cell (13, 14).

Nevertheless, structural features exist in the OHC that could potentially account for a voltage-dependent charge movement that coincidentally occurs during the mechanical activity of the OHC. The OHC plasmalemma is intimately associated with an adjacent cortical cytoskeleton composed

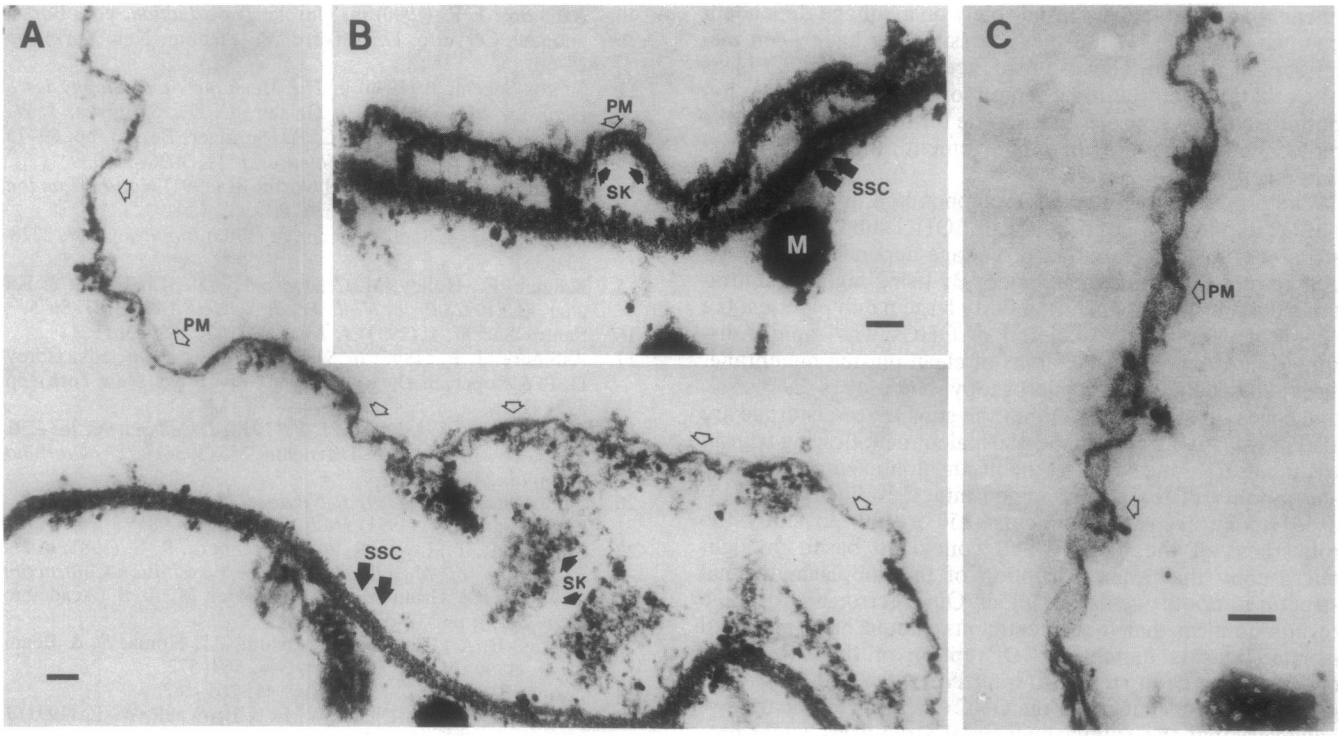

FIG. 6. Higher-magnification view of the same cell as in Fig. 5 at a different level. (*A*) Area in which the plasma membrane (PM) has peeled away from underlying structures. The subplasmalemmal cytoskeleton (SK) appears digested and has been freed from the intracellular aspect of the plasma membrane. As a result, the subsurface cisternae (SSC) are able to involute into the cell. In some cells there was evidence for cisternal vesiculation. (*B*) Area where the digestion process is in an early stage. Attachments between the plasma membrane and subsurface cisternae via the cytoskeleton are still visible. (*C*) At higher magnification, an area of plasma membrane fully clear of intracellular structures. (Bars = 100 nm.)

of circumferential actin filaments, cross-linked by spectrin (18). In addition, filamentous pillar processes extend from the plasma membrane to the circumferential filaments and subsurface cisternae (19), a membranous system whose surface area can be greater than that of the cell's plasma membrane. While the potential electrical interaction between subsurface cisternae and plasmalemma had been initially dismissed based on the observation that OHC capacitance could be accounted for by the linear dielectric properties of the OHC surface plasma membrane (2), subsequent experiments indicated that this was not the case (20). Clearly, it is now known that a portion of OHC capacitance is voltage dependent and can be of the same order of magnitude as the cell's linear capacitance (11, 12). Electrical interactions between two membranous systems could increase input capacitance, just as occurs during alterations of gap junctional communication in inner ear supporting cells (21). It is not inconceivable that the OHC plasma membrane could recruit cisternal membrane in a voltage-dependent manner, either through reversible membrane fusion or through some electrical interaction of the cisternae with the extracellular space, perhaps via the pillar processes spanning the region between plasma membrane and cisternal membrane.

Another potential generator of nonlinear charge movement might exist due to the restrictive subplasmalemma space, resulting in a series resistance between the OHC plasma membrane and axis core (9). For example, it has been suggested that the pillars or spectrin may be associated with the mechanical response in a charge-dependent manner (9, 18). Perhaps movement of these structures or transmembrane ionic flow into the restrictive subplasmalemmal space can generate capacitive-like charge movements measurable across the intracellular series resistance. Indeed, a residual nonlinear ionic conductance exits in the OHC even after substantial efforts to block voltage-dependent currents (12, 14). Simple circuits of skeletal muscle membranous systems have been envisioned that theoretically could generate nonlinear charge movement based solely on a voltage-dependent conductance (22). While these possibilities have been dismissed for muscle, because evidence of the molecular basis of excitation–contraction charge movement exists (23), hypotheses of this type are appropriate for the OHC, where the molecular basis of the charge movement remains uncharacterized.

The present experiments were conducted in order to rule out these potential contributions of OHC subplasmalemmal structures to the generation of voltage-dependent nonlinear charge movement or capacitance. By using high concentrations of trypsin (300 μg/ml) in fairly large patch pipettes, the subplasmalemmal cytoskeleton of OHCs was rapidly disrupted, leaving expansive areas of clean plasma membrane, as evidenced by electron microscopy. Not only is the restrictive space no longer present but the subsurface cisternae are also physically remote to the plasmalemma following trypsin treatment. Despite such treatment, the nonlinear capacitance and motility of the cell remained intact. Kalinec *et al.* (15) used similar trypsin treatments (150 μg/ml) to study the robustness of the motility and concluded based on light microscopy that after disruption of the subplasmalemmal structures motility remained intact. Our electron microscopic results confirm that their treatments should have provided isolated plasma membrane. Disruption of the subsurface cisternae has been shown to interfere with the normal longitudinal length changes of the OHC (24, 25). It is clear now, however, that the subplasmalemmal structures, while providing structural and other support for the normal OHC, do not contribute directly to the generation of gating currents or the underlying mechanical response of the plasma membrane. The only logical explanation for the persistence of the OHC's nonlinear capacitance is that it is intrinsic to the lateral plasma membrane, just as the mechanical response is. Furthermore, both sensor and effector appear to be protected from enzymatic digestion, possibly indicating that (*i*) the complex is proteinaceous and buried within the lipid bilayer, (*ii*) some sites of the proteinaceous complex are external to the bilayer but lack trypsin cleavage sites, (*iii*) portions of the complex external to the bilayer are digested but do not contribute significantly to sensor/motor activity, or (*iv*) the underlying mechanism is somehow lipid based.

Current theories of OHC motility envision molecular motors within the lateral plasma membrane, which change conformation upon sensing alterations in transmembrane voltage (15, 26, 27). The colocalization of sensor and effector, not only along the extent of the OHC's length (13, 14) but also within the plane of the OHC plasma membrane, may indicate that the densely packed intramembranous particles first observed nearly two decades ago (28) ultimately underlie the inner ear's remarkable sensitivity and frequency selectivity.

We thank Dr. Ilsa Schwartz, Patricia Eager, and Frank N. Tilley III. This research was supported by the National Institutes of Health-National Institute of Deafness and Other Communication Disorders (Grant DC00273).

1. Brownell, W. E., Bader, C. R., Bertrand, D. & de Ribaupierre, Y. (1985) *Science* **227**, 194–196.
2. Ashmore, J. F. (1987) *J. Physiol. (London)* **388**, 323–347.
3. Santos-Sacchi, J. & Dilger, J. P. (1988) *Hear. Res.* **35**, 143–150.
4. Santos-Sacchi, J. (1992) *J. Neurosci.* **12**, 1906–1916.
5. Iwasa, K. H. & Kachar, B. (1989) *Hear. Res.* **40**, 247–254.
6. Ruggero, M. A. (1992) *Curr. Opin. Neurobiol.* **2**, 449–456.
7. Kachar, B., Brownell, W. E., Altschuler, R. & Fex, J. (1986) *Nature (London)* **322**, 365–368.
8. Holley, M. C. & Ashmore, J. F. (1988) *Proc. R. Soc. London B* **232**, 413–429.
9. Ashmore, J. F. (1989) in *Mechanics of Hearing*, eds. Kemp, D. & Wilson, J. P. (Plenum, New York), pp. 107–113.
10. Ashmore, J. F. (1990) in *Sensory Transduction*, eds. Borsellino, A., Cervetto, L. & Torre, V. (Plenum, New York), pp. 25–50.
11. Santos-Sacchi, J. (1990) in *The Mechanics and Biophysics of Hearing*, eds. Dallos, P., Geisler, C. D., Mathews, J. W., Ruggero, M. A. & Steele, C. R. (Springer, Berlin), pp. 69–75.
12. Santos-Sacchi, J. (1991) *J. Neurosci.* **11**, 3096–3110.
13. Dallos, P., Evans, B. & Hallworth, R. (1991) *Nature (London)* **350**, 155–157.
14. Huang, G.-J. & Santos-Sacchi, J. (1993) *Biophys. J.* **65**, 2228–2236.
15. Kalinec, F., Holley, M. C., Iwasa, K. H., Lim, D. J. & Kachar, B. (1992) *Proc. Natl. Acad. Sci. USA* **89**, 8671–8675.
16. Santos-Sacchi, J. (1993) *J. Neurosci.* **13**, 3599–3611.
17. Ashmore, J. F. (1992) in *Sensory Transduction*, eds. Corey, D. P. & Roper, S. D. (Rockefeller Univ. Press, New York), pp. 395–412.
18. Holley, M. C. & Ashmore, J. F. (1990) *J. Cell Sci.* **96**, 283–291.
19. Flock, A., Flock, B. & Ulfendahl, M. (1986) *Arch. Otorhinolaryngol.* **243**, 83–90.
20. Santos-Sacchi, J. (1989) *J. Neurosci.* **9**, 2954–2962.
21. Santos-Sacchi, J. (1991) *Hear. Res.* **52**, 89–98.
22. Mathias, R. T., Levis, R. A. & Eisenberg, R. S. (1981) in *The Regulation of Muscle Contraction: Excitation-Contraction Coupling*, eds. Grinnell, A. D. & Brazier, M. A. B. (Academic, New York), pp. 39–52.
23. Adams, B. A., Tanabe, T., Mikami, A., Numa, S. & Beam, K. G. (1990) *Nature (London)* **346**, 569–572.
24. Evans, B. N. (1990) *Hear. Res.* **45**, 265–282.
25. Dieler, R., Shehata-Dieler, W. E. & Brownell, W. E. (1991) *J. Neurocytol.* **20**, 637–653.
26. Dallos, P., Hallworth, R. & Evans, B. N. (1993) *J. Neurophysiol.* **70**, 299–323.
27. Santos-Sacchi, J. (1993) *Biophys. J.* **65**, 2217–2227.
28. Gulley, R. L. & Reese, T. S. (1977) *Anat. Rec.* **189**, 109–124.